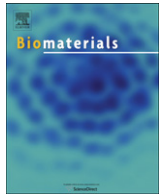




Contents lists available at ScienceDirect

Biomaterials

journal homepage: www.elsevier.com/locate/biomaterials

Craniofacial vertical bone augmentation: A comparison between 3D printed monolithic monetite blocks and autologous onlay grafts in the rabbit

Faleh Tamimi^{a,*}, Jesus Torres^b, Uwe Gbureck^c, Enrique Lopez-Cabarcos^d, David C. Bassett^a,
 Mohammad H. Alkhraisat^d, Jake E. Barralet^a

^a Faculty of Dentistry, McGill University, 3640 University Street, Montreal, H3A 2B2 QC, Canada

^b Health Science III, Rey Juan Carlos University, Alcorcon, Madrid, Spain

^c Department of Functional Materials in Medicine and Dentistry, University of Würzburg, Würzburg, Germany

^d Department of Physical Chemistry II, Universidad Complutense de Madrid, Spain

ARTICLE INFO

Article history:

Received 22 June 2009

Accepted 24 July 2009

Available online xxx

Keywords:

Monetite
 Autologous bone
 Autograft
 Onlay bone graft
 Monolithic blocks
 Histomorphometry

ABSTRACT

Onlay autografting is amongst the most predictable techniques for craniofacial vertical bone augmentation, however, complications related to donor site surgery are common and synthetic alternatives to onlay autografts are desirable. Recent studies have shown that the acidic calcium phosphates, brushite and monetite, are osteoconductive, osteoinductive and resorb faster *in vivo* than hydroxyapatite. Moreover, they can be 3D printed allowing precise host bone-implant specific conformation. The objectives of this study were to confirm that craniofacial screw fixation of 3D printed monetite blocks was possible and to compare the resulting vertical bone augmentation with autograft. 3D printed monolithic monetite onlay implants were fixed with osteosynthesis screws on the calvarial bone surface of New Zealand rabbits. After 8 weeks, integration between the implant and the calvarial bone surface was observed in all cases. Histomorphometry revealed that 42% of the monetite was resorbed and that the new bone formed within the implant occupied 43% of its volume, sufficient for immediate dental implant placement. Bone tissue within the autologous onlay occupied 60% of the volume. We observed that patterns of regeneration within the implants differed throughout the material and we propose that the cause was the anatomy and blood supply pattern in the region. Rapid prototyped monetite being resorbable osteoconductive and osteoinductive would appear to be a promising biomaterial for many bone regeneration strategies.

© 2009 Elsevier Ltd. All rights reserved.

1. Introduction

Advances in biomaterials and surgical techniques have contributed to an increase in the application of dental implants for the restoration of partially and totally edentulous patients. An important factor to predict the long-term success of osseointegrated implants is a sufficient volume of healthy bone at recipient sites [1]. However, this is frequently lacking as a result of trauma, tooth loss or infection such as advanced periodontitis [1].

Vertical alveolar bone loss in partially edentulous patients renders prosthetic rehabilitation difficult and presents a major challenge for dental implant placement due to anatomical restrictions and surgical difficulties. The nasal cavity, maxillary sinus and the mandibular inferior alveolar nerve limit the bone height available for implant placement. In addition a large empty space

between the maxillary and mandibular ridge complicates the final treatment outcome.

Clinical and histological data support the use of vertical ridge augmentation techniques to enable dental implant placement. The main approaches considered in clinical practice include guided bone regeneration (GBR) [1–10], distraction osteogenesis [11–20] and onlay bone grafts [21–27]. Table 1 summarizes the results of some of the most relevant articles in the literature regarding vertical bone augmentation. It is apparent that although distraction osteogenesis can produce significantly greater bone height than GBR and onlay bone grafting, there is a higher rate of complication associated with this technique. GBR appears to generate a similar amount of new bone to onlay bone grafting but carries a higher rate of complication.

The principles of GBR were applied in the early 1990s to atrophic jaws [2]. Severe vertical defects were treated by means of titanium reinforced non-resorbable barrier membranes in conjunction with titanium dental implants. Vertical ridge augmentation can be achieved successfully using GBR. However, success appears to be

* Corresponding author.

E-mail address: faleh.taminimarino@mail.mcgill.ca (F. Tamimi).

Table 1
Summary of clinical studies reporting the average bone height gained and complications rate of vertical bone augmentation by GBR, distraction osteogenesis and onlay autografts.

Surgical technique											
GBR				Distraction osteogenesis				Onlay bone graft			
Pts/graft no	ABH (mm)	Complcn (%)	Refs	Pts/site	ABH (mm)	Complcn (%)	Refs	Pts	ABH (mm)	Complcn (%)	Refs
5/6	4.0	16.7	[2]	10/13	7.5	23	[11]	25	4.22	4	[24]
6/6	4.95	16.7	[3]	7/10	7.0	30	[12]	9	2.2	0	[25]
1/1	2.5	0	[4]	14/14	10.3	14.3	[13]	8	4.6	25	[26]
2/2	ID	0	[5]	28/28	6.5	50	[14]	56	ID	7.1	[27]
18/22	Na	13.6	[6]	10/10	ID (6–8)	10	[15]				
20/22	5.02	18	[7]	37/37	9.9	21.6	[16]				
6/6	3.14	ID	[8]	10/10	ID	20	[17]				
1/1	ID	0	[9]	10/10	7.3	30	[18]				
7/10	3.15	10	[10]	7/7	ID (10–15)	28.6	[19]				
				37/45	8.2	75.7	[20]				
				10/10	6–12	20	[21]				
				10/10	5.3	70	[22]				
				11/11	6.1	27.3	[22]				
				9/9	5.3	33.3	[23]				
Pool ABH ± SD	4.3 ± 0.5	13.3 ± 15.5			8.0 ± 1.5	34.1 ± 24.6			3.9 ± 0.9	7.1 ± 8.8	

ABH: average bone height obtained; Pts: patients; Complcn: complications; Ref: references; SD: standard deviation. ID: insufficient data.

highly technique-sensitive and therefore application to a wide community of operators and clinical settings remains unclear [1–9]. Another major limitation of this technique appears to be the ability to regenerate bone only along the axis of the applied force [1,10–22].

Bone block onlay grafts were also introduced in the early 1990s to increase the vertical height of the maxilla and mandible [29]. This technique involves extracting a block of autologous bone from a donor site such as the iliac crest or the mandibular *ramus*, and fixing the block with osteosynthesis screws onto the recipient site. Onlay bone grafting appears to have acceptable results and minor complications at the recipient site; however, complications are often noted at the donor site. At this moment there is no satisfactory synthetic alternative to onlay autologous bone grafts for maxillofacial bone augmentation.

Synthetic calcium phosphates are excellent biomaterials for bone regeneration. However, the most commonly used calcium phosphates such as hydroxyapatite (HA) and β -tricalcium phosphate (β -TCP) have limited *in vivo* resorption and remodeling capacity, and are therefore unsuitable as onlay bone graft substitutes for vertical bone augmentation [30,31]. Recent studies have demonstrated the potential of dicalcium phosphate compounds with higher solubilities at physiological pH, in vertical bone augmentation procedures [32,33]. For instance, dicalcium phosphate dihydrate (brushite) application in the form of cements or granules has shown good potential for maxillofacial bone augmentation [32]. However, *in vivo*, brushite has a tendency to reprecipitate as insoluble HA slowing its replacement by bone. A closely related compound, dicalcium phosphate anhydrous (CaHPO_4) commonly known as monetite is slightly less soluble and appears not to transform to HA. It has recently been found to be osteoconductive and resorbable *in vivo* [34–36], which is of great interest for maxillofacial bone augmentation.

We have recently developed a 3D-powder printing technique enabling computer designed monetite blocks to be made easily for specific bone regeneration applications [34]. In this study we sought to answer two questions. Firstly would screw fixation of a printed bioceramic enable satisfactory osteointegration, and secondly, how would bone tissue behave following abutment with a monetite block.

2. Materials and methods

Onlay blocks were prepared using a previously described 3D printing technique [34]. Briefly, tricalcium phosphate (TCP) was synthesized by heating a mixture of

dicalcium phosphate anhydrous (CaHPO_4 , monetite) (Merck, Darmstadt, Germany) and calcium carbonate (CaCO_3 , calcite) (Merck, Darmstadt, Germany) in a 2:1 molar ratio to 1400 °C for 7 h followed by quenching to room temperature. The sintered cake was crushed with a pestle and mortar and passed through a 160 μm sieve. Subsequent milling of TCP was performed in a planetary ball mill (PM400, Retsch, Germany) for 10 min. Printing of cement samples was performed with a 3D-powder printing system (Z-Corporation, USA) using the TCP powder and diluted phosphoric acid (H_3PO_4) (Merck, Darmstadt, Germany) with concentration of 20 wt%. The implant design was drafted using CAD software (Alibre design Xpress 10.0). The samples were cylindrical tablets 9.0 mm in diameter, 2.0 mm thick, with a 0.5 mm central hole for fixation with osteosynthesis screws (Fig. 1). After printing, samples were removed from the powder bed, cleaned from residual unreacted TCP powder and stored in 20% H_3PO_4 for 3 × 60 s to increase the degree of reaction to DCPD. The blocks were then dehydrated into monetite (dicalcium phosphate anhydrous) and simultaneously sterilized by autoclaving (121 °C; humidity 100%; 30 min) (see Fig. 1A) [34,36]. The final phase composition of the samples was approximately 63% monetite and 37% unreacted TCP [34] with a total porosity of 44% and a compressive strength of 15 MPa.

Prior to implantation, X-ray diffraction (XRD) patterns of the materials were recorded using monochromatic $\text{CuK}\alpha$ radiation (D5005, Siemens, Karlsruhe, Germany). Data were collected from $2\theta = 20^\circ$ – 40° with a step size of 0.02° and a normalized count time of 1 s/step. The phase composition was checked by means of The International Centre for Diffraction Data reference patterns for α -TCP (PDF Ref. 09-0348), β -TCP (PDF Ref. 09-0169), monetite (PDF Ref. 09-0080) and brushite (PDF Ref. 09-0077). Post implantation, XRD patterns were recorded on poly-methyl-methacrylate (PMMA) embedded implants using the same method.

The implantation protocol was approved by the ethical committee for animal experiments of the Rey Juan Carlos University of Madrid. Experiments were conducted in accordance with the guidelines described by the European Communities Council Directive of 24 November 1986 (86/609/EEC), and adequate measures were taken to minimize pain and discomfort to the animals. Eight New Zealand rabbits (3.5–4.0 kg) were used for this study. The rabbits were anaesthetized, the head was shaved and the cutaneous surface was disinfected with povidone iodine solution prior to the operation. A ~5 cm long full depth incision was made on the *linea media* of the *calvaria* and the periosteum was separated from the bone surface with a periosteal elevator. A trephine burr was then used to cut two bilateral circular full thickness autograft cores (10 mm diameter) in the posterior part of the exposed cranium. The circular autologous onlay bone grafts (9.0 mm in diameter) and the monetite blocks were secured with osteosynthesis titanium screws (AO/ASIF 4.0 self-drilling screws; Synthes, Synthes GmbH&Co, Umkirch, Germany) side by side on the anterior part of the exposed cranium (Fig. 1).

The incision was closed with a silk 3-0 suture and the animals were sacrificed after 8 weeks. Histological examinations were performed on dehydrated and resin embedded sections. Briefly, explants were fixed in 2.5% glutaraldehyde solutions and dehydrated in ascending concentrations of ethanol. The samples were then pre-infiltrated for 24 h and infiltrated with resin for another 24 h before embedding in polymerization resin at -20°C for 14 days (Technovit, Leica Microsystems GmbH Wetzlar, Germany). Following embedding, histological sections were taken using a micro saw (Leica Microsystems GmbH, Wetzlar; Germany), and the samples were stained with methylene blue (MB) and basic fuchsin (BF). Un-implanted monetite blocks were also resin embedded to be analyzed as well by optical and electronical microscopy.

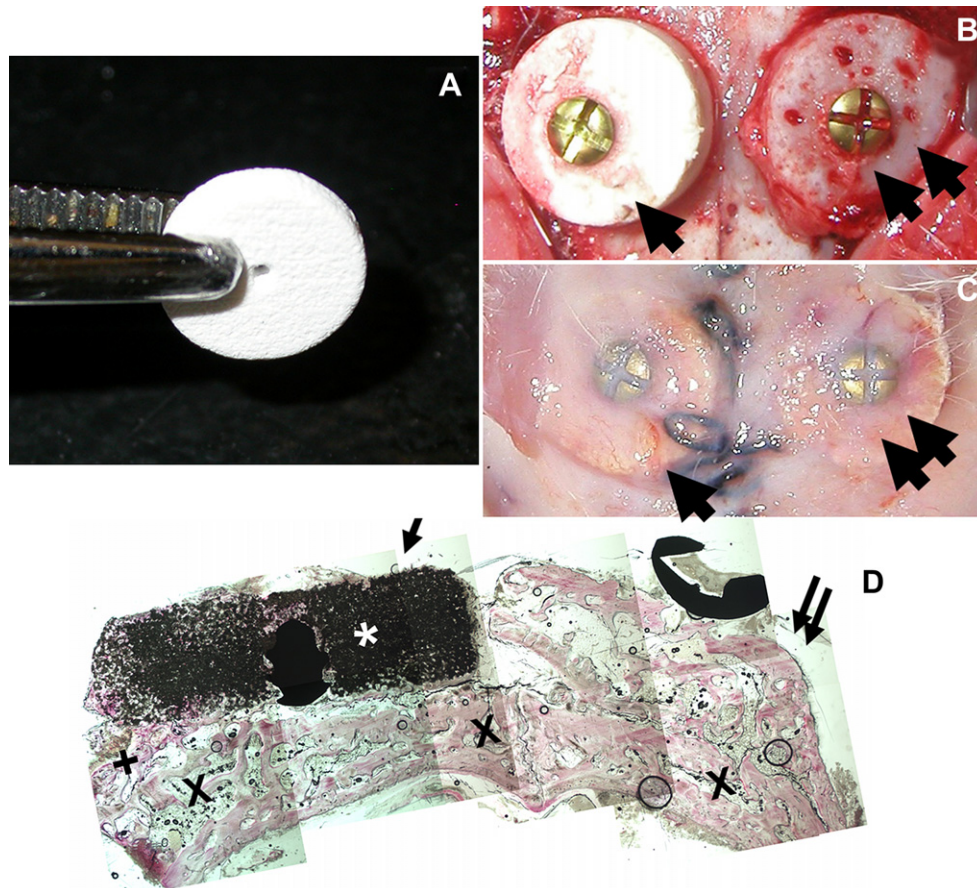


Fig. 1. A: Photograph of a 3D printed monetite discs. B: Surgical fixation of the monetite block (1 arrow) and the autologous block (2 arrows) over the rabbit calvaria with osteosynthesis screws. C: Exposure of the implant site at post mortem surgical extraction after 8 weeks of implantation. D: Histological micrographs of a coronal section from the bone explant sites stained with BF/MB (pictures were taken at an original magnification of $\times 5$). The sections show the original bone calvarium (X), the remaining monetite block (*) and the bone augmentation free of remaining unresorbed monetite (+).

Electron microscopy was used to examine cement microstructure with a Hitachi S3000-N VP-SEM (Hitachi-HT, Wokingham, Berkshire, UK) operating at an accelerating voltage of 20 kV. The resin embedded sections were sputter coated with gold-palladium alloy prior to electron beam analysis at high vacuum. Backscattered electron micrographs (BSE-SEM) were taken, and energy dispersive X-ray (EDX) analysis was performed using an Oxford detector and INCA software (Oxford Instruments, Abingdon, Oxfordshire, UK).

The optical histological observations were used to perform the histomorphometric analysis of the implant area, to calculate the percentage of bone and remaining material within the augmented tissues. The area of augmented bone was divided in smaller areas to performed localized histomorphometrical analysis. Interpolation of the localized histomorphometric values was used to depict the average distribution of bone within the implants and to provide a statistical mapping of the histological sections [37] (Origin 7.0; Origin Lab Co.; Northampton; MA). The augmented area was obtained from the interpolation analysis, and the percentage of monetite onlay resorption was calculated by subtracting the remaining graft size and area percentage from the block size and porosity before implantation.

A two-way ANOVA for paired samples was used to evaluate differences between the onlay graft materials and original calvarial bone. Statistical significance was set at a value of $p < 0.01$.

3. Results

3.1. Clinical observations

No complications were noted during the fixation of onlay implants (Fig. 1B) and the animals healed normally. Upon implant recovery, no signs of rejection were apparent for either the monetite or the autologous onlay implants and both appeared to be

integrated and vascularized (Fig. 1C). Moreover, no loosening of the screws or blocks was observed.

3.2. Histological observations

Upon histological coronal observation, the autologous onlay implants could be differentiated from original bone surface by the localized over-contouring created on the calvaria (Fig. 1D). Moreover, they were completely integrated to the original bone surface. The thickness of the autologous implants became thinner on the lateral side with less bone volume than the original surfaces. The monetite onlay blocks were well integrated to the calvarial surface (Fig. 1), partially resorbed and substituted by newly formed bone (Fig. 1, [+]). Resorption of monetite and subsequent replacement by new bone were more pronounced on the lateral sides of the implants as well as on the surfaces in direct contact with the calvarial bone surface. Bone conduction was observed not only along the implants' periphery but within the micropores.

At higher magnification, the remaining unresorbed monetite blocks appeared to be highly porous (Fig. 2A). These pores were often filled with newly formed bone throughout the remaining implant (Fig. 2B). The amount of new bone formed within the implant increased in sites in which the implant was in contact with native bone. Direct contact between newly formed bone and remaining monetite was observed around and within the implants, indicating osteoconductive properties of monetite in vertical bone augmentation (Fig. 2C). Furthermore, at the bone-implant

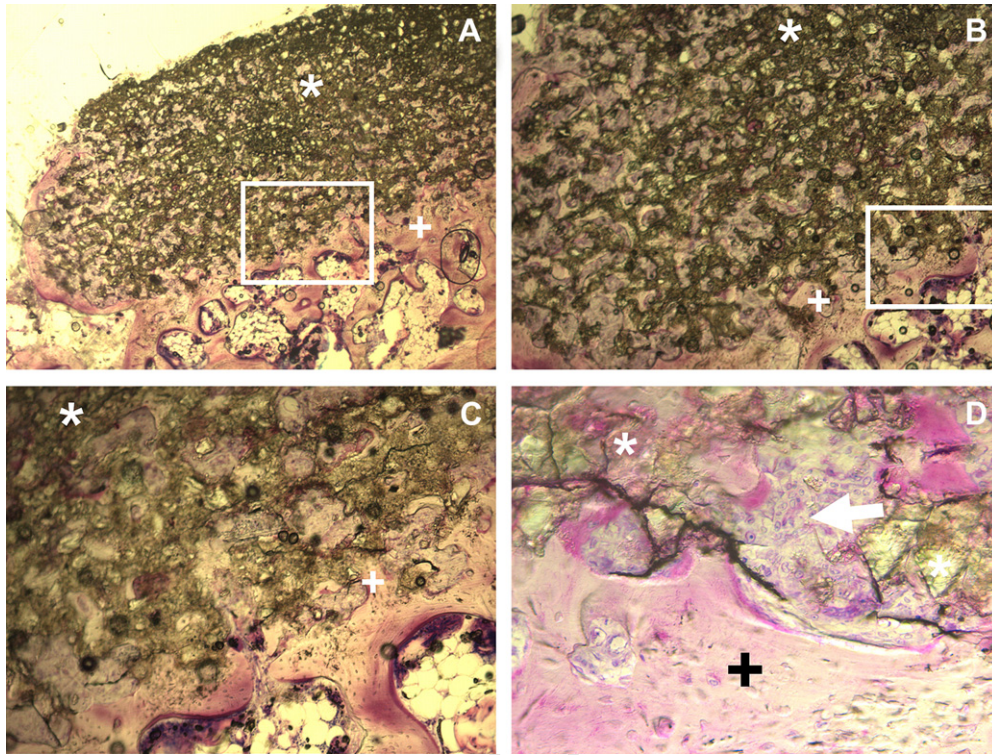


Fig. 2. Micrograph of a monetite implant after 8 weeks implantation taken at: original magnification $\times 2.5$ and a field width 5.0 mm (A); original magnification $\times 5$ and a field width 2.5 mm (B); and original magnification of $\times 10$ and a field width 1.2 mm (C); Remaining monetite biomaterial (*) can be observed to be infiltrated with newly formed bone (+). At original magnification $\times 20$ and field width 0.6 mm (D) cellular activity at the bone-implant interface was apparent (arrow). Sections were stained with BF/MB.

interface, bone formation and the appearance of cells with a morphology suggestive of osteoblasts were also strong evidence in support of the osteoconductive properties (Fig. 2D).

Histological observation of the autologous bone graft onlays revealed a high degree of resorption within the augmented bone tissues. Osteoclast activity was observed on the external surface of the onlay as well as within the autologous block itself (Fig. 3).

3.3. SEM analysis

BSE-SEM cross-section micrographs of the un-implanted monetite blocks revealed a dense porous structure (Fig. 4A–C). After implantation, the remaining unresorbed monetite block could be easily differentiated from the original bone surface and from the calcified newly formed bone using BSE-SEM (Fig. 4D–F). The remaining monetite appeared lighter grey than the newly formed bone (Fig. 4D). Isolated sites of new bone formation could be observed away from the original bone surface indicating good osteoconductive properties (Fig. 4E). At high magnification osteocyte lacunae could be observed within the remaining graft matrix, confirming the presence of calcified bone within the onlay implant, in close contact with the remaining monetite matrix (Fig. 4F).

EDX analysis of the bone-implant interface revealed that at specific sites, the concentrations of calcium and phosphate within the remaining matrix were similar to those of the original calvarial bone (Fig. 4G–I), confirming the presence of bone within the monetite matrix. Moreover, EDX mapping confirmed the presence of high concentrations of phosphate (Fig. 4I) within the unresorbed implant matrix. X-ray diffraction patterns of the blocks after implantation confirmed the composition of unresorbed graft material in the blocks after implantation to be monetite and β -TCP (Supplemental data).

3.4. Bone height analysis

Direct vertical bone height measurements were not possible due to the variability in the anatomical convexity of the calvarial surface. Therefore ratio measurements between the autologous and monetite blocks were calculated from the histological sections crossing both implants' centre. The ratio between the height measurements were taken every 2 mm across the implants' sections by measuring the distance between the inner cranial surface and the highest bone tissue formed in the implant. Histo-morphometric analyses indicated that the maximum increase in bone height over the original bone surface was similar in both onlay grafts (autologous bone and monetite) (Fig. 5A). However, in the distal areas the bone height obtained with monetite blocks was higher than with autografts, while in the medial area the bone height obtained with autografts was higher than with monetite blocks. Since it was apparent that the amount of bone formation varied from medial to lateral locations, bone volume was assessed at the top, centre and bottom regions of the graft every 2 mm across the sections where the central screw hole was visible.

3.5. Histomorphometry

Bone and remaining material could be observed within the onlay autografts and monetite blocks. The percentage of mineralized bone and remaining bone graft material for both onlay grafts are presented in Fig. 5B. The amount of mineralized tissue (remaining material + bone) was much higher in monetite implants ($91.3 \pm 13.1\%$) than in autologous implants ($60.1 \pm 6.0\%$) ($p < 0.01$). In contrast the percentage of bone volume within the monetite blocks ($43.4 \pm 8.1\%$) was lower than that of the autologous onlays ($p < 0.01$). However, this difference was rather small, probably due to the high degree of internal resorption of the autologous

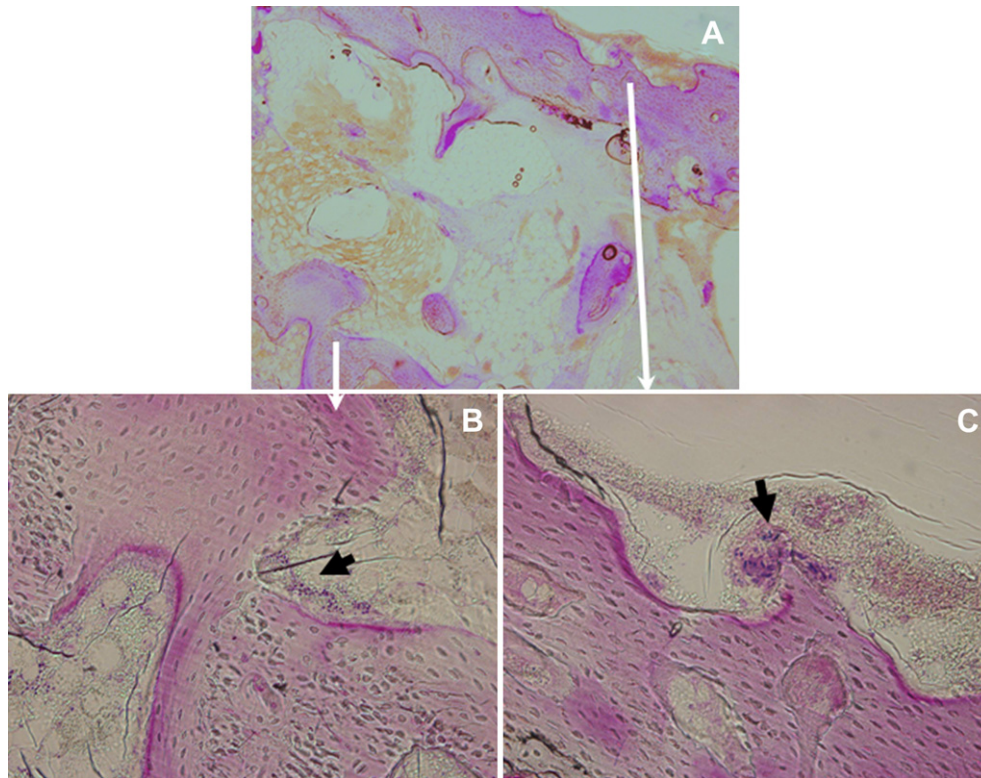


Fig. 3. A: Histological micrograph of autologous onlay bone graft showing large areas of resorbed bone (original magnification $\times 5$; field width 2.5 mm). B: Multinuclear cell activity was evident within the graft trabecula; and C: on the external onlay surface (original magnifications $\times 20$; field width 0.6 mm).

grafts. Indeed, the bone area within autografts was lower than the original calvarial bone ($72.3 \pm 9.2\%$) (Fig. 5B). The degree of resorption of the monetite onlay block throughout the implantation period was calculated by subtracting the histomorphometrical area of un-implanted monetite blocks, from the percentage of remaining material after implantation, and it was found to be $42.3 \pm 17.1\%$ (Supplemental data).

Histomorphometrical analyses at specific smaller areas of the cross-sections revealed that bone growth was heterogeneous within both onlay materials (Fig. 6). The percentage of bone formed within the onlay autologous grafts was higher at the lateral end and superior surface whereas very little bone was measured close to the calvarial surface on the medial side (Fig. 6). In contrast bone growth within the monetite blocks was lower on its superior surface, but there was also significant bone growth on the lateral side of the graft proximal to the calvarium. Surprisingly, on the medial side proximal to the calvarium the amount of new bone obtained with monetite onlays was significantly greater than that obtained with autologous grafts ($p < 0.01$).

4. Discussion

In this study, using 3D printed monetite onlay blocks, we were able to obtain similar values of vertical bone augmentation as those observed with autologous onlay bone grafts [24–26] while simultaneously avoiding complications associated with autologous bone extraction.

4.1. Screw fixation

Monetite-based biomaterials have recently shown great potential as bone substitutes in terms of osteoconductive,

osteoinductive and resorption properties [34–36]. In this study, we confirm the materials osteoconductive and bioresorbative properties in craniofacial vertical bone augmentation. However, mechanical stability of bone grafts is essential for successful bone regeneration treatments [1]. The monetite printed blocks appeared to be well integrated to the original bone surface, indicating that screw fixation of these 3D printed ceramics is possible, allowing predictable bone augmentation results.

4.2. In vivo resorption

The high porosity inherent in monetite bioceramics produced through rapid prototyping was likely to enhance the biological behavior observed. Moreover, it was interesting to observe that the porosity increased throughout the material after implantation, indicating a bulk resorption. The monetite blocks conducted new bone formation throughout its surface, and the high porosity left behind by the resorbed material allowed significant bone infiltration within the implant matrix. In addition, the high rate of resorption is likely to provide a localized concentration of phosphate and calcium ions that would aid in the mineralization and bone formation process [30,31]. Monetite resorption appeared to be more pronounced on the implant–bone interface, and on the lateral margin of the implant, probably due to better perfusion in those areas.

4.3. Bone augmentation

The bone height gained with monetite blocks was comparable to that obtained with autologous bone and the volume of newly formed bone around and within the remaining implant material was $43.4 \pm 8.1\%$. Dental implants can be successfully placed into

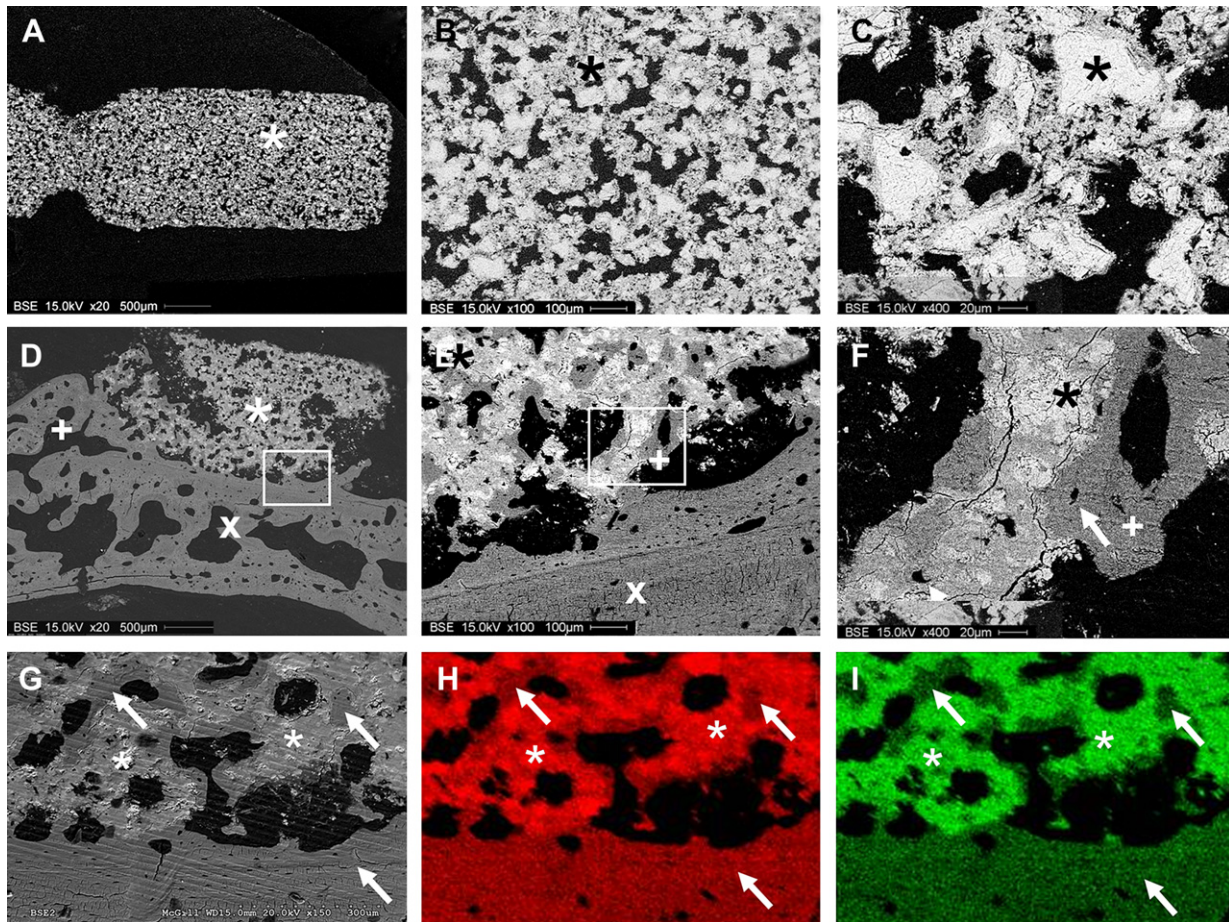


Fig. 4. BSE-SEM picture of monetite block before implantation at original magnification $\times 20$ (A), $\times 100$ (B) and $\times 400$ (C). BSE-SEM picture of monetite block implanted on the calvarial bone. D: At lower magnification ($\times 10$) new bone (+) was observed to grow around the remaining monetite block (*) over the original bone calvarial surface (x). E: At higher magnification ($\times 100$) new bone (+) was observed to grow within the monetite matrix (*). F: At magnification $\times 400$ the presence of micropores resembling osteocyte lacunae (arrows) confirmed the presence of bone growing within the remaining unresorbed monetite matrix (*). Bone-implant interface was analyzed by SE-SEM (G) and EDX elemental analysis mapping for calcium (H) and phosphorous (I). The arrows indicate bone tissue in the original bone surface and within the remaining implant, while stars reveal the remaining unresorbed monetite matrix.

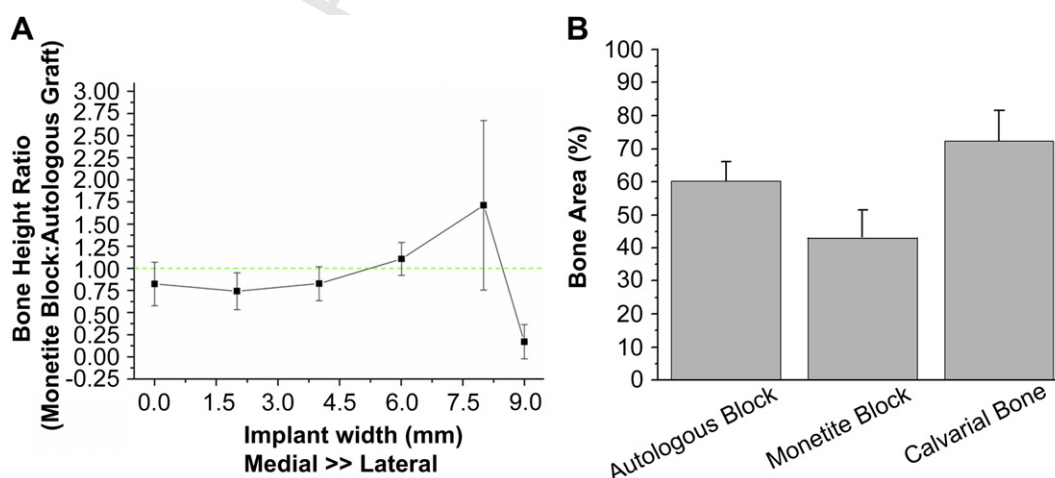


Fig. 5. A: Histomorphometric measurement of maximum bone height gained, the data are presented as the ratio between the maximum bone heights gained with monetite blocks to the maximum bone heights gained with autologous grafts, as a function of distance to the *linea media*. No significant differences were found between the vertical bone heights gained with either only graft material. B: Histomorphometric measurements of mineralized tissue volume depicting percentage of bone volume (light grey); and percentage of remaining graft volume (dark grey), within the area treated with autologous blocks, and monetite blocks, as well as within the original calvarial bone. (*) Augmented bone volume significantly lower than in autologous bone only ($p < 0.01$).

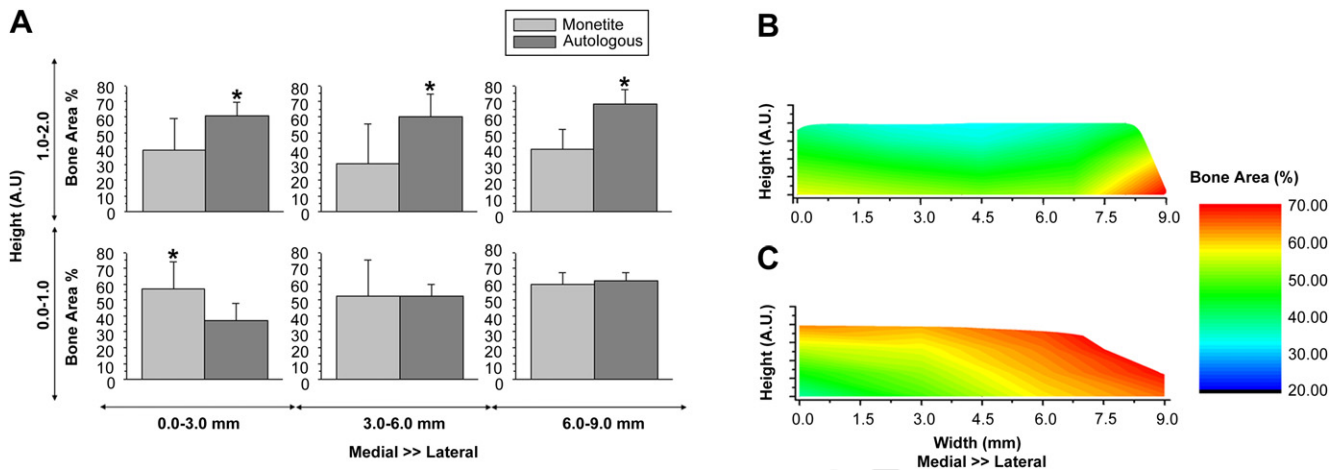


Fig. 6. A: Histomorphometric measurements of mineralized tissue volume depicting the average bone area percentage within 6 equal size segments of the autologous and monetite blocks in cross-section (* significant differences $p < 0.01$). B and C: Interpolation mapping of average bone area percentage (from Figure 11A) throughout the onlay implants' cross-section.

regenerated bone with a bone volume of 30–40% [38]. Therefore the volume of bone obtained using monetite onlay implants is likely to be enough to support titanium implants, although further studies should be conducted to evaluate the stability of dental implants in augmented bone using this procedure in the maxillofacial region.

4.4. 3D printed bioceramics

Computer design and printing of bone substitutes allows the fabrication of custom made designs for specific applications. In previous studies 3D printed brushite and monetite blocks have been used to study the phenomena of osteoinduction [36] and angiogenesis [34] of bone substitutes *in vivo*. In this study, 3D printed monetite blocks were successfully used in craniofacial vertical bone augmentation onlays, indicating new possibilities to custom make 3D printed blocks for onlay grafts in the maxillofacial region.

Bone augmentation procedures have to ensure good mechanical stability of the graft material in order to obtain adequate bone growth and avoid fibrous tissue encapsulation [38,39]. To this end rigid fixation of maxillofacial bone grafts is essential to provide mechanical support and minimize micro-movement during the initial healing phase. To overcome mechanical instability, granular graft materials have been secured to the bone surface with membranes or titanium meshes, while autologous onlay grafts are usually fixed with osteosynthesis screws [2–27]. The 3D printed design of our monetite blocks included a hole to allow fixation on the calvarial bone surface with osteosynthesis screws. This design provided good onlay implant stability and may have played an important role in obtaining the excellent vertical bone augmentation and integration achieved by this technique.

Recently synthetic polyethylene blocks have been used as onlay implants by fixing them with titanium screws in maxillofacial defects [41]. However these onlays can only be used for soft tissue support in ophthalmologic and aesthetic applications, as they lack the capacity to bear the load of functional forces. Even though monetite blocks have a lower compressive strength than cortical bone, their compressive strength resembles that of spongy bone (9.4–25.2 MPa) [42]. Currently, spongy bone is widely used for maxillofacial bone augmentation procedures in areas receiving masticatory loads; therefore the properties of our monetite blocks may be adequate as an alternative to screwed autologous onlay in these kinds of interventions. Moreover, bone ingrowth within the

implants is likely to increase their mechanical performance over time.

4.5. An alternative to autografts?

In this comparative study, autologous grafts performed better than monetite onlays overall, however monetite onlay grafts were able to obtain similar and even better results in specific regions within the onlays. The vertical bone height gained with monetite onlays was similar to that obtained with autografts, and even superior to it at the lateral end of the onlays. Moreover, the percentage of new bone growth within the calvarial surface of the monetite onlays was similar to that obtained with autologous bone grafts, and greater in the medial region. This difference highlights the great potential of resorbable osteoconductive biomaterials may have in vertical bone augmentation procedures, since the areas showing greater bone growth were also the areas where less remaining graft was observed.

4.6. Effect of anatomy

Histological observations and histomorphometrical analyses revealed that autografts resorbed more on the medial calvarial surface and on the lateral superior surface of the graft, while monetite blocks appeared to resorb on the lateral end of the implant. Bone conduction was more pronounced on the lateral side of both the monetite and autologous onlays. These regional variations in resorption and mineralization may have arisen due to the vascular anatomy of the calvarial bones since the major supply to the calvaria is provided by the middle meningeal artery and its branches while the majority of the outer surface of the craniofacial skeleton is supplied by tiny perforators from the overlying periosteum [43]. In both cases, the direction of arterial blood flow is towards the *linea media*; therefore the lateral sides are better irrigated than the medial portions. Additionally the stretching of the periosteum to accommodate the implants may have compromised the blood supply of the *linea media* by creating sub-cutaneous pressure and limiting bone augmentation in that area. Significant resorption of the autologous onlay was expected since resorption and remodeling of implanted bone with limited functionality are well documented [44]. A large amount of resorption may have caused a reduction in the bone volume and bone height gained, so that the real performance of the autologous bone may well be much more comparable to that of the monetite onlays.

In this study, the potential of monetite onlay blocks as bone graft substitute in onlay augmentation procedures was demonstrated. The 3D printing technique was employed to produce blocks that can be easily adapted to produce variable shapes and geometries [34,36,46]. Therefore it is plausible that refinement of the monetite monolith geometrical design used here may be possible to further improve performance, and in the clinic be used to create custom made implants. Future studies should be focused on optimizing new bioresorbable materials and techniques for onlay bone augmentation in maxillofacial surgery, and to evaluate the capacity of the augmented bone to support osteointegrated dental implants.

5. Conclusions

This study has demonstrated that 3D printed monetite blocks designed for vertical bone augmentation can be directly fixed to bone surfaces using osteosynthesis screws. Onlay grafts of 3D printed monetite blocks achieved levels of vertical bone augmentation similar to those of autologous bone grafts in a rabbit calvarial model. These findings demonstrate that a new type of synthetic onlay bone grafting material may be applied as an attractive alternative to autologous onlay bone grafting in maxillofacial surgery.

Uncited references

[28,40,45,47,48].

Acknowledgments

The authors acknowledge financial support from "Fundacion Espanola para la Ciencia y Tecnologia" (FECYT); The Spanish Science and Education Ministry (MAT2006-13646-C03-01); the UCM Program for Research Groups; The Canada Research Chair program and NSERC Discovery Grant (J.E.B.), and the Québec Ministère des Relations Internationales (Québec-Bavaria Exchange Program) PSR-SIIRI-029 IBI.

Appendix

Figures with essential colour discrimination. Figs. 1–6 in this article are difficult to interpret in black and white. The full colour images can be found in the online version, at doi:10.1016/j.biomaterials.2009.07.049.

Appendix. Supplementary data

Supplementary data associated with this article can be found in the online version, at doi:10.1016/j.biomaterials.2009.07.049.

References

- [1] Rocchietta I, Fontana F, Simion M. Clinical outcomes of vertical bone augmentation to enable dental implant placement: a systematic review. *J Clin Periodontol* 2008;35(8 Suppl.):203–15.
- [2] Simion M, Trisi P, Piattelli A. Vertical ridge augmentation using a membrane technique associated with osseointegrated implants. *Int J Periodont Rest* 1994;14:496–511.
- [3] Tinti C, Parma-Benfenati S, Polizzi G. Vertical ridge augmentation: what is the limit? *Int J Periodont Rest* 1996;16:220–9.
- [4] Piattelli M, Scarano A, Piattelli A. Vertical ridge augmentation using a resorbable membrane: a case report. *J Periodontol* 1996;67:158–61.
- [5] Tinti C, Parma-Benfenati S, Manfrini F. Spacemaking metal structures for nonresorbable membranes in guided bone regeneration around implants. Two case reports. *Int J Periodont Rest* 1997;17:53–61.
- [6] Tinti C, Parma-Benfenati S. Vertical ridge augmentation: surgical protocol and retrospective evaluation of 48 consecutively inserted implants. *Int J Periodont Rest* 1998;18:434–43.

- [7] Simion M, Jovanovic SA, Trisi P, Scarano A, Piattelli A. Vertical ridge augmentation around dental implants using a membrane technique and autogenous bone or allografts in humans. *Int J Periodont Rest* 1998;18:8–23.
- [8] Parma-Benfenati S, Tinti C, Albrektsson T, Johansson C. Histologic evaluation of guided vertical ridge augmentation around implants in humans. *Int J Periodont Rest* 1999;19:424–37.
- [9] Canullo L, Trisi P, Simion M. Vertical ridge augmentation around implants using e-PTFE titanium-reinforced membrane and deproteinized bovine bone mineral (Bio-Oss): a case report. *Int J Periodont Rest* 2006;26:355–61.
- [10] Simion M, Fontana F, Raperini G, Maiorana C. Vertical ridge augmentation by expanded-polytetrafluoroethylene membrane and a combination of intraoral autogenous bone graft and deproteinized anorganic bovine bone (Bio-Oss). *Clin Oral Implants Res* 2007;18:620–9.
- [11] Klug CN, Millesi-Schobel GA, Millesi W, Watzinger F, Ewers R. Preprosthetic vertical distraction osteogenesis of the mandible using an L-shaped osteotomy and titanium membranes for guided bone regeneration. *J Oral Maxillofac Surg* 2001;59:1302–8.
- [12] McAllister BS. Histologic and radiographic evidence of vertical ridge augmentation utilizing distraction osteogenesis: 10 consecutively placed distractors. *J Periodontol* 2001;72:1767–79.
- [13] Rachmiel A, Srouji S, Peled M. Alveolar ridge augmentation by distraction osteogenesis. *Int J Oral Maxillofac Surg* 2001;30:510–7.
- [14] Jensen OT, Cockrell R, Kuhike L, Reed C. Anterior maxillary alveolar distraction osteogenesis: a prospective 5-year clinical study. *Int J Oral Maxillofac Surg* 2002;31:67–78.
- [15] Raghoobar GM, Liem RS, Vissink A. Vertical distraction of the severely resorbed edentulous mandible: a clinical, histological and electron microscopic study of 10 treated cases. *Clin Oral Implants Res* 2002;13:558–65.
- [16] Chiapasco M, Consolo U, Bianchi A, Ronchi P. Alveolar distraction osteogenesis for the correction of vertically deficient edentulous ridges: a multicenter prospective study on humans. *Int J Oral Maxillofac Implants* 2004;19:399–407.
- [17] Chiapasco M, Romeo E, Casentini P, Rimondini L. Alveolar distraction osteogenesis vs. vertical guided bone regeneration for the correction of vertically deficient edentulous ridges: a 1–3-year prospective study on humans. *Clin Oral Implants Res* 2004;15:82–95.
- [18] Kunkel M, Wahlmann U, Reichert TE, Wegener J, Wagner W. Reconstruction of mandibular defects following tumor ablation by vertical distraction osteogenesis using intraosseous distraction devices. *Clin Oral Implants Res* 2005;16:89–97.
- [19] Iizuka T, Hallermann W, Seto I, Smolka W, Smolka K, Bosshardt DD. Bi-directional distraction osteogenesis of the alveolar bone using an extraosseous device. *Clin Oral Implants Res* 2005;16:700–7.
- [20] Enislidis G, Fock N, Millesi-Schobel G, Klug C, Wittwer G, Yorit K, et al. Analysis of complications following alveolar distraction osteogenesis and implant placement in the partially edentulous mandible. *Oral Surg Oral Med O* 2005;100:25–30.
- [21] Türker N, Basa S, Vural G. Evaluation of osseous regeneration in alveolar distraction osteogenesis with histological and radiological aspects. *J Oral Maxillofac Surg* 2007;65:608–14.
- [22] Schleier P, Wolf C, Siebert H, Shafer D, Freilich M, Berndt A, et al. Treatment options in distraction osteogenesis therapy using a new bidirectional distractor system. *Int J Oral Maxillofac Implants* 2007;22:408–16.
- [23] Chiapasco M, Zaniboni M, Rimondini L. Autogenous onlay bone grafts vs. alveolar distraction osteogenesis for the correction of vertically deficient edentulous ridges: a 2–4-year prospective study on humans. *Clin Oral Implants Res* 2007;18:432–40.
- [24] Bahat O, Fontanelli RV. Implant placement in three-dimensional grafts in the anterior jaw. *Int J Periodont Rest* 2001;21:357–65.
- [25] Cordaro L, Amadei DS, Cordaro M. Clinical results of alveolar ridge augmentation with mandibular block bone grafts in partially edentulous patients prior to implant placement. *Clin Oral Implants Res* 2002;13:103–11.
- [26] Chiapasco M, Zaniboni M, Rimondini L. Autogenous onlay bone grafts vs. alveolar distraction osteogenesis for the correction of vertically deficient edentulous ridges: a 2–4-year prospective study on humans. *Clin Oral Implants Res* 2007;18:432–40.
- [27] Barone A, Covani U. Maxillary alveolar ridge reconstruction with non-vascularized autogenous block bone: clinical results. *J Oral Maxillofac Surg* 2007;65(10):2039–46.
- [28] McCarthy JG, Schreiber J, Karp N, Thorne CH, Grayson BH. Lengthening the human mandible by gradual distraction. *Plast Reconstr Surg* 1992;89:1–8.
- [29] Isaksson S, Alberius P. Maxillary alveolar ridge augmentation with onlay bone grafts and immediate endosseous implants. *J Craniomaxillofac Surg* 1992;20:2–7.
- [30] Dorozhkin SV. Calcium orthophosphates. *J Mater Sci* 2007;42(4):1061–95.
- [31] Bohner M. Calcium orthophosphates in medicine: from ceramics to calcium phosphate cements. *Injury* 2000;31(S4):37–47.
- [32] Tamimi F, Torres J, Lopez-Cabarcos E, Bassett DC, Habibovic P, Luceron E, et al. Minimally invasive maxillofacial vertical bone augmentation using brushite based cements. *Biomaterials* 2009;30(2):208–16.
- [33] Mariño FT, Torres J, Tresguerres I, Jerez LB, Cabarcos EL. Vertical bone augmentation with granulated brushite cement set in glycolic acid. *J Biomed Mater Res A* 2007;81(1):93–102.
- [34] Gbureck U, Hölzel T, Klammert U, Würzler K, Müller FA, Barralet JE. Resorbable calcium phosphate bone substitutes prepared by 3d powder printing. *Adv Funct Mater* 2007;17(18):3940–5.

- 1021 [35] Tamimi F, Torres J, Kathan C, Baca R, Clemente C, Blanco L, et al. Bone
1022 regeneration in rabbit calvaria with novel monetite granules. *J Biomed Mater*
1023 *Res A* 2008;87A(4):980–5.
- 1024 [36] Habibovic P, Gbureck U, Doillon CJ, Bassett DC, van Blitterswijk CA, Barralet JE.
1025 Osteoconduction and osteoinduction of low-temperature 3D printed bio-
1026 ceramic implants. *Biomaterials* 2008;29(7):944–53.
- 1027 [37] Renka RJ, Cline AK. A triangle-based C^1 interpolation method. *Rocky Mountain*
1028 *J Math* 1984;14:223–37.
- 1029 [38] Hallman M, Sennerby L, Lundgren S. A clinical and histologic evaluation of
1030 implant integration in the posterior maxilla after sinus floor augmentation
1031 with autogenous bone, bovine hydroxyapatite, or a 20:80 mixture. *Int J Oral*
1032 *Maxillofac Implants* 2002;17(5):635–43.
- 1033 [39] Freihofer HP. Stability after osteotomy of the edentulous maxilla. *J Cranio-*
1034 *maxillofac Surg* 1989;17(7):306–8.
- 1035 [40] Cottrell DA, Wolford LM. Long-term evaluation of the use of coralline
1036 hydroxyapatite in orthognathic surgery. *J Oral Maxillofac Surg* 1998;56(8):935–
41. discussion 941–2.
- [41] Eski M, Sengezer M, Turegun M, Devci M, Isik S. Contour restoration of the
secondary deformities of zygomaticorbital fractures with porous poly-
ethylene implant. *J Craniofac Surg* 2007;18(3):520–5.
- [42] De Santis R, Ambrosio L, Nicolais L. Mechanical properties of tooth structures. 1037
In: Barbucci R, editor. *Integrated biomaterials science*. New York, US: Springer; 1038
2002. p. 589–99.
- [43] Cutting CB, McCarthy JG, Berenstein A. Blood supply of the upper craniofacial 1039
skeleton: the search for composite calvarial bone flaps. *Plast Reconstr Surg* 1040
1984;74(5):603–10.
- [44] Schortinghuis J, de Jong JR, Paans AM, Ruben JL, Raghoobar GM, Stegenga B, 1041
et al. The influence of barrier membranes on autologous bone grafts. *J Dent* 1042
Res 2008;87(11):1048–52.
- [45] Galea LG, Bohner M, Lemaître J, Kohler T, Müller R. Bone substitute: trans- 1043
forming beta-tricalcium phosphate porous scaffolds into monetite. *Biomateri-* 1044
als 2008;29(24–25):3400–7.
- [46] Bohner M, Gbureck U. Thermal reactions of brushite cements. *J Biomed Mater* 1045
Res B Appl Biomater 2008;84(2):375–85.
- [47] Gbureck U, Vorndran E, Müller FA, Barralet JE. Low temperature direct 3D 1046
printed bioceramics and biocomposites as drug release matrices. *J Control* 1047
Release 2007;122:173–80.
- [48] Meyer U, Büchter A, Wiesmann HP, Joos U, Jones DB. Basic reactions of 1048
osteoblasts on structured material surfaces. *Eur Cell Mater* 2005; 1049
9:39–49. 1050
1051
1052